RSC Advances

This article can be cited before page numbers have been issued, to do this please use: D. AGGOUN, A. OURARI and W. DERAFA, *RSC Adv.*, 2015, DOI: 10.1039/C5RA10819E.

ROYAL SOCIETY OF CHEMISTRY

www.rsc.org/advances

View Article Online
DOI: 10.1039/C5RA10819E

A novel copper (II) complex with unsymmetrical tridentate-Schiff base: Synthesis, Crystal structure, Electrochemical, Morphological and Electrocatalytic behaviors toward electroreduction of alkyl and aryl halides

Ali OURARI*, Wassila DERAFA, Djouhra AGGOUN*

Laboratoire d'Electrochimie, d'Ingénierie Moléculaire et de Catalyse Redox (LEIMCR), Faculté de Technologie, Université Ferhat ABBAS Setif-1, Route de Béjaia, Setif 19000-Algeria.

Abstract

This work describes the synthesis of a new unsymmetrical tetradentate copper (II) Schiff base complex **Cu(L)(Py)(ClO_4)**containing N_3O donor atoms. The tridentate ligand (**HL**) has been prepared by condensation of dehydroacetic acidon 1,2-diaminopropane in methanol. The reaction of the ligand with an appropriate amount of copper (II) perchlorate hexahydrate (1:1 ratio) in the same solvent and in the presence of an excess of pyridine (Py) yields the title compound. The tridentate ligand (**HL**) with pyridine act as mixed ligands where three nitrogen and an enolic oxygen atoms were chelated to the copper centre.This complex has been fully characterized by FT-IR, UV-Vis spectrophotometry, and cyclic voltammetry. Single crystal X-ray diffraction of this complex showed that the copper ion was coordinated by one ligand, one pyridine molecule with one perchlorate anion in a square pyramidal geometry. The **Cu(L)(Py)(ClO_4)** complex crystallizes in an orthorhombic system, space group of -Pcab with a = 11.051, b = 15.58, c = 21.736Å and Z = 8. The electrochemical reduction of copper (II) complex, in N,N-dimethylformamide(DMF) solvent using cyclic voltammetry, produces conducting polymeric films on different electrode substrates, such as glassy carbon (GC), indium tin oxide (ITO) and fluorine tin oxide (FTO). The catalytic activity of this complex in homogeneous and heterogeneous electrocatalytic media seems to be efficient for the electroreduction of bromocyclopentane and iodobenzene.

KEY WORDS: *Copper (II) complex, X-ray diffraction, Modified electrodes, Electrocatalysis, Alkyl and aryl halides.*

*Corresponding authors. Tel.: +213 776 28 15 33; fax: +213 36 61 11 54 (A. Ourari). Tel.: +213.697.78.81.45.
E-mail addresses: alourari@yahoo.fr (A. OURARI); agghafida@gmail.com (Dj. AGGOUN).

View Article Online
DOI: 10.1039/C5RA10819E

1. Introduction

Among many organic reagents currently used in coordination chemistry, Schiff bases have been increasingly developed in their different aspects. In general, they are prepared in high yield using one step procedure via condensation of common aldehydes or ketones with amines [1]. In coordination chemistry**,** these kinds of ligands belonging to the bidentate, tridentate and tetradentate Schiff base ligands are considered highly interesting and desirable compounds owing to their exceptional characteristics, notably easy preparation procedures, versatile structures and diverse physical and chemical properties [1].This class of compounds and their transition metal complexes has been studied extensively with the aim of shedding light on various aspects ofelectrocatalysis[2], corrosion protection [3], biosensors [4] and in many important biological activities, such as antitumoral, antifungal, and antibacterial activities [5].

As an example of starting ketones, dehydroacetic acid is a powerful material which is involved in the synthesis of several heterocyclic compounds [6] and chelating agents such as those of Schiff bases. These ligands are also usually used in the synthesis of Schiff base complexes of transition metals [7]. In addition, it was shown that the heterocyclic compounds resulting from this starting material occupied a dominating positionin coordination chemistry research that explores some therapeutic and pharmacological activities [8] and is useful in the treatment of human diseases as well.

Thus, Schiff base complexes develop an important catalytic activity under homogeneous and heterogeneous conditions, particularly in oxidation reactions, such as those mimicking cytochromes P-450 enzymes [9]. Considering their low cost and large availability, other transition metal complexes have also been used as catalysts for a wide variety of reactions, including olefin polymerization[10], molecular oxygen and carbon dioxide reduction [11,12]. As for tetradentate transition metal complexes containing two oxygen and two nitrogen (OONN) as donor atoms, they have attracted the attention of many researchers [13] due to their structural versatility and electronic properties which can be fine-tuned by choosing an appropriate amine and salicylaldehyde derivatives judiciously substituted [14]. In fact, the reductive electro-polymerization of diverse complexes has been investigated [15] and the electrochemical design of modified electrodes by electrodeposition of polymer films has also been extensively developed.In addition, copper (II) Schiff base complexes have also aroused a

View Article Online
DOI: 10.1039/C5RA10819E

wide interest because they possess a diverse spectrum of biological and pharmaceutical activities. Copper (II) is known to form complexes with a variety of molecular geometries (e.g., tetrahedral, square planar, square pyramidal, and octahedral). Furthermore, copper complexes have been copiously studied because of their structural, catalytical and good magnetic properties.

As part of our ongoing research into the design and synthesis of a new copper Schiff base complex, a family of heterocyclic ligand is being presented here which isderived from dehydroacetic acid, 1,2-diaminopropane, pyridine and copper perchlorate hexahydrate in a methanolic solution. This complex was formed in one pot with only one azomethine (–$C(CH_3)$=N–) group yielding an unreacted amino group of 1,2-diaminopropane leading to an acceptable yieldunder mild conditions.

In this case, we notice that the ring of dehydroacetic acid does not appear to be open during the reaction as it was reported in the literature **[16]**, particularly in the presence of nucleophile agents such as pyridinic derivatives. This behavior may be due to an inhibition of the nucleophilic effect of pyridine since the reaction was conducted in a methanolic solution at room temperature and without reflux. Finally, the resulting compound was confirmed by crystallographic studies as discussed further and the structure of this copper (II) Schiff base complex was illustrated by the following Scheme 1.

«Scheme 1»

2. Experimental

2.1.Physical Measurements

All solvents and chemical were of reagent grade and were purchased from Aldrich and Fluka. They were used as received without any further purification. The solvents were dried before use with the appropriate drying reagents. IR spectra were recorded on Perkin and Elmer 1000-FT-IR Spectrometer using KBr disks, while the electronic spectra (UV-Vis) were obtained on a Unicam UV-300 Spectrophotometer having 1 cm as a path length cell. Electrochemical experiments were performed on a voltalab 40, Potentiostat galvanostat controlled by microcomputer. Thus, the cyclic voltammograms were recorded after compilation of electrochemical data obtained with an individual cell of 5 ml, using a conventional three-

View Article Online
DOI: 10.1039/C5RA10819E

electrode system in DMF solutions containing 0.1M tetra-n-Butylammonium perchlorate (TBAP) and 0.001 M copper complex. The electrodes were polished by diamond paste and copiously rinsed with acetone and then by DMF. The working electrode was either a disc of glassy carbon (diam. 3 mm) or a semi-transparent electrode of indium tin oxide (ITO, Resistance=50 Ω, thickness= 100 nm) while the counter electrode was a platinum wire, and all potentials were expressed versus the saturated solutions of calomel electrode (SCE). ITO- and FTO-electrodes were typically prepared by cutting the glass to suitable size (active area = 1 cm^2).

The X-ray photoelectron spectroscopy (XPS) measurements were carried out in a MULTILAB 2000 (THERMO VG) spectrometer equipped with an Al K _X-ray source (1486.6 eV). Survey and high resolution spectra were recorded in constant pass energy mode (100 and 20 eV, respectively). The CASAXPS program with a Gaussian–Lorentzian mix function and Shirley`s background subtraction was employed to deconvolute the XP spectra. The C 1s peak at 284.6 eV was used to correct charging effects.

2.2.X-ray Crystallography

Colorless crystals of **Cu(L)(Py)(ClO_4)** suitable for X-ray diffraction were obtained by slow evaporation from methanol solution. A single crystal was mounted on a APEXII, Bruker-AXS diffractometer, Mo-Kα radiation (λ = 0.71073 Å), *T* = 150(2) K; *Centre de Diffractométrie (CDFIX), Université de Rennes1*, France. The structure was solved by direct methods using the *SIR97* program **[17]**, and then refined with full-matrix least-square methods based on F^2 (*SHELXL-97*) **[18]** with the aid of the *WINGX* **[19]** program. All non-hydrogen atoms were refined with anisotropic atomic displacement parameters. H atoms were finally included in their calculated positions.Crystal data and refinement results are given in Table 1 and complete crystallographic results are further given as supplementary materials.

2.3. Synthesis

Synthesis of complex Cu(L)(Py)(ClO_4)

Synthesis of copper complex was carried out via known chemical reactions, as depicted in Scheme 1. So, this complex was obtained by mixing stoechiometric quantities of dehydroacetic acid 0.168 g (1 mmol) with 0.075 g (1 mmol) of 1,2-diaminopropane in methanol solution (10 ml). To this mixture was added an excess of pyridine (2mmol, 158mg) and then copper perchlorate hexahydrate 0.370 g (1 mmol) was similarly dissolved in the

View Article Online
DOI: 10.1039/C5RA10819E

same medium. After two hours of reaction, a blue precipitate was observed and recovered by filtration. It was purified by successive cleaning steeps using cooled methanol and diethyl ether and then dried over $CaCl_2$ giving 72% as yield. Its suitable single crystals were obtained by slow evaporation.

3. Results and discussion

The synthesized copper complex is stable in air and moisture. Its solubility is usually good in the coordinating solvents such as acetonitrile, DMF and DMSO.

3.1. Spectral characterization

- ***Infrared Spectra***

The IR spectrum of the copper complex shows two absorption bands at 3345 and 3297 cm^{-1}. These absorption bands are attributed to the $\nu_{(NH2)}$ vibration [20]. Also, another band with a moderate intensity was observed at 1691cm^{-1} and ascribed to the vibration $\nu_{(O=C-O)}$ of the lactone function. The strong and sharp absorption band due to the azomethine $\upsilon_{C=N}$ group of the Schiff base appears at 1649 cm^{-1} [21]. The complex shows a band at 1089 cm^{-1} suggesting the presence of perchlorate as counter anion [22]. In addition, bands observed at 1457 and 1352 cm^{-1} are assigned respectively to the vibration of coordinated phenolic Cu–O–C stretching mode and the Cu–N stretching $\nu_{(C—N)}$. The formation of the M–O and M–N bonds were further supported by the appearance of the ν(M–O) and ν(M–N) bands in the regions 439-520 and 624-670 cm^{-1}, respectively [23]. This indicates that phenolic oxygen and azomethine nitrogen atoms are involved in coordination.

- ***Electronic Spectra***

The formation of the copper (II) complex was also confirmed by UV-Vis spectrum. The electronic spectrum of **Cu(L)(Py)(ClO_4)**, recorded in DMF solutions, displays its most important features between 300 and 370 nm. The intense absorption band observed at 310 nm arose from a transition involving electron migration along the entire conjugate system of the ligand associated with the C=N linkages (n–π*) [24]. The weak band at near 368 nm can be attributed to the L→M charge transfer transition [25]. The electronic transitions, observed in the visible region around 620 nm, are ascribed to the weak d–d transitions [26].

View Article Online
DOI: 10.1039/C5RA10819E

3.2.Crystallographic Study

The **Cu(L)(Py)(ClO_4)** crystallizes in the orthorhombic space group Pcab with 8 formula units in the cell. The asymetric unit of copper complex, and the atomic numbering used, is illustrated in **Fig. 1**. Relevant X-ray diffraction data and selected bond lengths and angles are listed respectively in tables 1 and 2. The Cu^{II} ion is five-coordinated in a square-pyramidal geometry by three of the four donors of the Schiff base complex (a nitrogen atom from the amino group, a second nitrogen atom from the imino group and an oxygen atom of the pyranone molecular residue), the fourth donor is the pyridine nitrogen atom. The coordination around the metal ion is completed by a longer axial bond with the perchlorate O atom of perchlorate unit. The bond lengths for the coordination Cu^{II} sphere range from 1.970 (3)to 2.036 (3)Å and 2.538 (2) Å for Cu-N and Cu-O distances respectively. These results are in good agreement with similar compounds described in the literature **[27,28]**. Cisoid and transoid angles for Cu deviate from their ideal values of 90° and 180° and are found to be in the range 85.43 (11)– 95.38 (11)° and 172.95 (11)– 174.51 (11)°, respectively (**Table 2**).The bond lengths and angles around C24 are also in agreement with sp^3 hybridization of this atom. The azomethine relationship is evident from the N14–C20 bond length (1.475 (4)) and the C10–N14–C20 bond angle (120.4 (3)). All H atoms attached to C or N atoms were positioned geometrically and treated as riding on their parent atoms with C-H = 0.95 Å ($C_{aromatic}$), 0.98 Å (C_{methyl}) and 0.92 Å (NH2) with $U_{iso}(H) = 1.2\ U_{eq}(C_{aromatic,\ NH2})$ or $1.5\ U_{eq}(C_{methyl})$. The trigonality index $\boldsymbol{\tau}$= (174.51 – 172.95)/60 = 0.026 indicating that the complex has a nearly perfect planar tetragonal geometry [O12-Cu-N13 = 174.51° and N4-Cu-N14 = 172.95°] **[29]**.

«Figure 1»

«Table 1»

«Table 2»

3.3.Electrochemical Study

3.3.1. Cyclic voltammetry

View Article Online
DOI: 10.1039/C5RA10819E

The redox properties of the monomer **Cu(L)(Py)(ClO_4)** 10^{-3} M were studied by cyclic voltammetry in DMF solutions containing 10^{-1}M of TBAP using 100 mVs^{-1} as scan rate after bubbling for more than 15 minutes under nitrogen atmosphere. The cyclovoltammograms, recorded in the range between 0.0 and +1.6V (**Fig. 2**, curve **A**), showed a redox couple at $E_{1/2}$ = 0.415V exhibiting respectively two waves Cu (III) at 0.55 V and Cu (II) species at 0.28V/SCE. The peak-to-peak separation (ΔEp) was found to be equal to 270 mV. The theoretical value of ΔEp for one-electron process is equal or slightly superior to 60 mV **[30]**. The large difference between the theoretical value and the experimental one would be due to a quasi-reversible behavior of the Cu (III)/Cu (II) redox couple. This indicates a relative slow redox transition and/or electron exchange process at the interface between the electrode and Cu (III)/Cu (II) metallic redox centers **[31]**, which implies that these electrochemical processes are mainly diffusion-controlled. In addition, in the range from -0.2 to -1.6V, it can be observed that the copper (II) complex shows a quasi-reversible redox system of the Cu (II)/Cu (I) at $E_{1/2}$ equal to -0.87 V/SCE and the peak-to-peak separation (ΔEp=140mV) **(Fig. 2**, curve **B)**.

«Figure 2»

3.3.2. Modified electrode poly-[Cu(L)(Py)(ClO_4)]/GC

In general, a modified electrode (ME) is prepared by electropolymerization of a monomer in two steps. Firstly, the monomer is electrodeposited as polymer either by repetitive cycling or by electrolysis at controlled potential. Secondly, when the modified electrode is obtained, it was copiously rinsed with bi-distilled water, with DMF and then transferred into another fresh electrolytic DMF solution no containing monomer. This ME was identified by an electrochemical method as cyclic voltammetry giving electrochemical characteristics of polymer, attesting the presence of the complex in the polymeric matrices.

On the anodic side, **Fig. 3** (Curve **A**) shows the evolution of cyclovoltammograms of **Cu(L)(Py)(ClO_4)** complex in DMF solutions at a scan rate of 100 mV s^{-1}. The cycling between -0.2 and 1.2 V/SCE exhibits a continuous increasing in ip_a and ip_c peak currents characterizing Cu (III)/Cu (II) redox couple where the electrodeposited films are more and more conductive. Moreover, as the number of scans increases, the anodic and cathodic peak currents shifted to more positive and more negative potentials respectively. This is consistent with an increase of the polymer thickness causing an increase in its electrical resistance. This

View Article Online
DOI: 10.1039/C5RA10819E

fact indicates that the copper complex is deposited onto the GC electrode surface and the modified electrode poly-**[Cu(L)(Py)(ClO_4)]**/GC is so obtained.

On the cathodic side, **Fig. 3** (Curve **B**) shows obviously that the electropolymerization reaction of **Cu(L)(Py)(ClO_4)** is easily performed by repetitive cycling from 0.0 to -1.2 V at scan rate of 50 mV s^{-1} with GC-electrode. The buildup of the poly-**[Cu(L)(Py)(ClO_4)]** films can be characterized by the increase in the ip_a and ip_c peak currents occurring in each repeated cycling which induces the deposition of a conductive polymer on GC-electrode surface **[32-34]**.

«Figure 3»

In this context, we have investigated the scan rate dependence for Cu (II)/Cu (I) redox couples in homogeneous and heterogeneous phases with their solution and solid phase respectively. Thus, a wide range of scan rates was explored starting from 25 to 500 mVs^{-1} (See **Fig. 4**). In addition, it can be seen that the redox currents increase with the increasing of scan rates and the potential values of anodic waves shift to the more positive potentials and the cathodic peak currents shift also towards the more negative potentials as the scan rates increase **[35]**. This phenomenon can be explained by the presence of the electroactive species in the bulk of the polymer requiring more energy.

«Figure 4»

3.3.3. Scanning electron micrographs

Transparent conducting oxide films are frequently used with substrates in developing electronics and optoelectronic devices, due to their conductive and optical properties. Among these substrates, fluorine-doped tin oxide and indium tin oxide deposited as thin films on glass stand out in the development of solar cells by their high electrical conductivity, optical transparency to visible radiation and low cost. Actually, it is possible to find studies focused on metal complexes films deposited on FTO or ITO substrates. Some authors show that the surface of the ITO and FTO film undergoes chemical and morphological changes during electrochemical treatment, affecting the electric and optic properties of the original substrate **[36]**. In this paper, we examine the morphological characteristics of FTO and ITO films during electropolymerization.

View Article Online
DOI: 10.1039/C5RA10819E

The modification of these two electrodes, poly-**[Cu(L)(Py)(ClO_4)]**/ITO and poly-**[Cu(L)(Py)(ClO_4)]**/FTO are elaborated in experimental conditions similar to those mentioned above for GC-modified electrodes. These modified electrodes are also copiously rinsed with bi-distilled water, with DMF and then transferred into another fresh electrolytic DMF solution containing no monomer. These MEs were identified by SEM microscopy (**Fig.5**).

This technique was used in order to evaluate the morphological and chemical changes occurringon the ITO- (**Fig.5 ABCD**) and FTO-electrode surfaces (**Fig.5 EFGH**). Thus, it was revealed that the presence of electrolyte salt gave rise to the formation of a number of remarkably different sizes of microparticles, as can be observed from SEM micrographs of poly-**[Cu(L)(Py)(ClO_4)]** films with ITO and FTO (See **Fig.5 A-G**). A typical fractal-like or dendritic structures consisting of a long central backbone and sharp side branches showing a preferential growth along two definite directions was observed as reported in the literature **[37,38]**. In our case, a difference between ITO and FTO SEM images was noticed suggesting that the ITO image shows the formation of crystalline structure **[36,37]**, while with FTO image, it exhibits microstructures of cube-shaped uniform-sized grains.

«Figure 5»

3.3.4. XPS Characterization

X-ray photoelectron spectroscopy (XPS) was used to examine the surface composition of **[Cu(L)(Py)(ClO_4)]** and poly-**[Cu(L)(Py)(ClO_4)]/ITO**. XPS spectra of Cu sample reveal the presence of chlorine, oxygen, carbon, nitrogen and Cu either in the **[Cu(L)(Py)(ClO_4** powder or in the poly-**[Cu(L)(Py)(ClO_4)]** film **(Fig. 6)**. Based on these analyses, copper is present approximately at the same level in both cases (Cu free and Cu-poly). Some kinetic energy shifts were observed for poly-**[Cu(L)(Py)(ClO_4)]/ ITO** (**Fig. 6b**) comparing to free copper **[Cu(L)(Py)(ClO_4)]** (**Fig. 6a**) (XPS). So, figures 7a and 7b shows wide-scan X-ray photoelectron spectra of **[Cu(L)(Py)(ClO_4)]** and poly-**[Cu(L)(Py)(ClO_4)]**/ITO electrode. The Cu coverage is clearly higher in **[Cu(L)(Py)(ClO_4)]** than in poly-**[Cu(L)(Py)(ClO_4)]**/ITO. The spectrum of the **[Cu(L)(Py)(ClO_4)]**/ITO sample shows large C 1s and O 1s contributions, weak Cu 2p and Cu Auger signals being also apparent. This indicates that the electrode surface is covered with a layer of **[Cu(L)(Py)(ClO_4)]**. In agreement with this, there is contribution from the ITO substrate which is supported by the present ITO composition (Si 2p, In 3p, Sn 3p). The narrow-scan Cu 2p spectra of the above-mentioned samples (**Fig. 6a**

View Article Online
DOI: 10.1039/C5RA10819E

and 6b) show the main Cu $2p_{3/2}$ and Cu $2p_{1/2}$ signals (They appearing at 934, and at 940 eV respectively) **[39-41]**. The **2p** electron BEs of the metals and the values for the carbon 1s, nitrogen 1s, oxygen 1s, and chlorine 2p electron BEs are given in survey spectrum A and B.

3.3.5. Reduction of bromocyclopentane and iodobenzene

Transition metals complexes have been extensively studied as catalysts for the reduction and synthesis of organic compounds **[42]**. When alkyl halides are directly elctroreduced, the resulting products via alkyl radical coupling and disproportionations as well as an abstraction of a hydrogen atom from the solvent by an alkyl radical **[43]**. As example of the literature **[44]**, the electroreduction of 1-bromooctane using nickel(I)-salen as catalyst yields *n*-octyl radical that can be involved in three reactions: (1) coupling to give *n*-hexadecane; (2) abstraction of a hydrogen atom from DMF to produce *n*-octane; (3) disproportionation to give *n*-octane and 1-octene **[44]**.

3.3.5.1.Effect of concentration

The electropolymerized films of poly-(**Cu(L)(Py)(ClO_4)**) and its monomer form were found to be efficient for the electrocatalytic reduction of alkyl and aryl halide compounds such as bromocyclopentane and iodobenzene in homogeneous and heterogeneous media.

So, the cyclic voltammogram, obtained in homogeneous phase presented in **Fig. 7 A**, shows a large enhancement in the reduction peak current ip_c of the metal center when the copper species are involved in the electroreduction of bromocyclopentane. This is consistent with an obvious electrocatalytic process. Indeed, these increased peak currents cannot be due to the direct reduction of the bromocyclopentane since they are formally occurring at a more negative potential value under the same experimental conditions. So, without catalyst the bromocyclopentane is electroreduced at -2.5V/SCE whereas in the presence of a catalyst its electroreduction occurs at very low potential values (-0.95V/SCE). The difference between the two potential values corresponds to a significant gain in potential (ΔEp = 1.55 V) attesting an important electrocatalytic effect as it can be observed with the peak currents of their Cu (II) /Cu (I) redox system (**Fig. 7 A**) **[45]**.

Also, the electropolymerized films of poly-(**Cu(L)(Py)(ClO_4)**) were found to be effective for the electrocatalytic reduction of bromocyclopentane and iodobenzene. Cyclic voltammograms obtained on glassy carbon electrode, coated with a polymerized film of poly-(**Cu(L)(Py)(ClO_4)**) in DMF solution, are illustrated in figure **7 B** and **C**. The same remarks

View Article Online
DOI: 10.1039/C5RA10819E

are observed confirming the presence of a significant electrocatalytic effect in the case of the modified electrodes with heterogeneous catalysis.

«Figure 7»

3.3.5.2.Scan rate effect

Fig. 8 shows the effect of scan rates for the electroreduction of iodobenzene. It can be clearly seen that there is an increase in the peak currents i_{pa} and i_{pc} of the redox system Cu (II)/Cu (I) accompanying the increase of the scan rates. So, these cyclovoltammograms were recorded in the presence of 5.10^{-3} M of iodobenzene using the poly-(**Cu(L)(Py)(ClO_4)**) as a modified electrode. This figure shows that the increase of the scan rate induces a shift of iodobenzene reduction potentials. These potential values were shifted to more cathodic values suggesting that this electrocatalytic behavior is in good accordance with a slow electrochemical process for an heterogeneous reduction reaction of iodobenzene using a **Cu(L)(Py)(ClO_4)** modified electrode.

«Figure 8»

In our case, the catalytic reduction of the alkyl halide leads probably to the production of a dimer (dicyclopentyl) with a good yield **(Way 1)**, cycloalkane **(Way 2)** and cycloalkene **(Way 3)** **[46]**. These processes take place in small yields either via disproportionation of alkyl radicals or via abstraction of a hydrogen atom from the solvent by an alkyl radical (**Scheme 2**).

«Scheme2»

Scheme 3 presents a set of mechanism reactions, showing different steps in which are involved the donor effects of protons governing the catalytic reduction of an alkyl monohalide. These chemical processes take into consideration the possibility of the electroreduction of one electron of copper (II) complex, that offer ways for alkylation of the imino bonds (C=N) of copper (II) complex during these processes. These facts can be summarized in the mechanism proposed by P.W. Raess *et al*. **(Scheme 3)** **[46]**.

View Article Online
DOI: 10.1039/C5RA10819E

«Scheme3»

Scheme 4 provides a sequence of pathways for the copper (II) complex catalyzing reduction of iodobenzene [47].

«Scheme4»

3.3.6. Chronoamperometry

Chronoamperometry results obtained for the two concentrations of iodobenzene solutions using poly-**Cu(L)(Py)(ClO_4)** are shown in Fig. 9. This technique can be employed to estimate the catalytic rate constant, k_h for the reaction between iodobenzene and poly-**Cu(L)(Py)(ClO_4)** according to Galus method [48].

$$\frac{Ic}{I} = \gamma^{1/2}[\sqrt{\pi} erf\sqrt{\gamma} + \frac{exp^{-\gamma}}{\sqrt{\gamma}}] \quad \text{Eq. 1}$$

$$\frac{Ic}{I} = \gamma^{1/2}\pi^{1/2} = \pi^{1/2}(k_h C_b t)^{1/2} \quad \text{Eq. 2}$$

Where $I_C$is the catalytic current of iodobenzene and poly-**Cu(L)(Py)(ClO_4)**, I_L is the limiting current in the absence of iodobenzene, and $\gamma = k_h C_b t$ (C_b is the bulk concentration of iodobenzene) is the argument of the error function. In the cases where **γ** exceeds two (2), the error function is almost equal to unity (1) and therefore, the above equation Eq. 1 can be reduced to the Eq. 2 where t is the time elapsed in seconds. This equation can be used to calculate the rate constant of the catalytic process k_h, based on the slope of I_C / I_L vs. $t^{1/2}$ plot, k_h can be obtained for a given iodobenzene concentration from the values of the slopes. An average value of k_h was found to be $k_h = 0{,}48\ 10^3\ cm^3 mol^{-1}\ s^{-1}$. This value also explains the sharp feature of the catalytic peak observed for the catalytic reduction of iodobenzene at the surface of **Cu(L)(Py)(ClO_4)** modified electrode.

«Figure 9»

4. Conclusion

By way of conclusion, a new unsymmetrical copper (II) Schiff base complex was synthesized by a simple and efficient method. The structure of this compound was confirmed by different

View Article Online
DOI: 10.1039/C5RA10819E

techniques, such as infrared spectroscopy, UV-Vis spectrophotometry analysis and also by cyclic voltammetry. In addition, molecular structure of the copper (II) complex was confirmed by XRD diffraction analysis. This complex was easily electropolymerized by cathodic reduction to its poly-**[Cu(L)(Py)(ClO_4)]** films yielding modified electrodes on which catalytic sites of copper as Cu(II) ions were identified in their coordinated forms. These new modified electrodes were found to be as efficient homogeneous and heterogeneous electrocatalysts for the reduction of bromocyclopentane and iodobenzene. These new materials can be used as modified electrodes in many applications, such as catalysis, electrocatalysis, electroanalysis and as well as sensors.

Aknowledgement

We gratefully aknowledge the "*Direction Générale de Recherche (DGR)"* for their financial support. The authors would like to thank Professor Spyridon Zafeiratos for his helpful discussions, *ICPEES, UMR 7515 du CNRS-Université de Strasbourg, ECPM, 25 Rue Becquerel, F-67087 Strasbourg Cedex 8, France* and Professor ZERROUAL Larbi, *Département Génie des procédés, Faculté de Technologie, Université Ferhat ABBAS Setif-1, Sétif 19000* Algeria.

References

[1] M. Aslantas, E. Kendi, N. Demir, A. E. Sabik, M. Tumer, M. Kertmen, Synthesis, spectroscopic, structural characterization, electrochemical and antimicrobial activity studies of the Schiff base ligand and its transition metal complexes, Spectro. chim. Acta, Part A., 74 (2009) 617-624.

[2] A. Adhikari, S. Radhakrishnan, R. Patil, Influence of dopant ions on properties of conducting polypyrrole and its electrocatalytic activity towards methanol oxidation, Synth. Met., 159 (2009) 1682-1688.

[3] M. Rizzi, M. Trueba, S.P. Trasatti, Polypyrrole films on Al alloys: The role of structural changes on protection performance, Synth. Met., 161 (2011) 23-31.

[4] D.D. Ateh, A. Waterworth, D. Walker, B.H. Brown, H. Navsaria, P. Vadgama, Impedimetric sensing of cells on polypyrrole-based conducting polymers, J. Biomed. Mater. Res., Part A.83A (2007) 391-400.

View Article Online
DOI: 10.1039/C5RA10819E

[5] T. Rosu, E. Pahontu, C. Maxim, R.Georgescu, N. Stanica, A. Gulea, Some new Cu(II) complexes containing an ON donor Schiff base: Synthesis, characterization and antibacterial activity, Polyhedron, 30 (2011) 154-162.

[6] E.S. Azam, A.F. EL Husseiny, H.M. Al-Amri, Synthesis and photoluminescent properties of a Schiff-base ligand and its mononuclear Zn(II), Cd(II), Cu(II), Ni(II) and Pd(II) metal complexes, Arabian J. Chem., 5 (2012) 45-53.

[7] A.H. Kianfar, W.A. K. Mahmood, M. Dinari, M. H. Azarian, F. Z. Khafri, Novel nanohybrids of cobalt (III) Schiff base complexes and clay: Synthesis and structural determinations, Spectro. chim. Acta Part A, 127(2014) 422-428.

[8] T. Punniyamurthy, S.J.S. Kalra, J. Iqbal, Cobalt(II) catalyzed biomimetic oxidation of hydrocarbons in the presence of dioxygen and 2-methylpropanal, Tett. Lett., 36 (1995) 8497-8500.

[9] J.P. Collman, T.R. Halbert, K.S. Suslick, T. Spiro, (ed.) Metal Ion Activation of Dioxygen, Wiley Interscience; New-York (1980).

[10] J. N. Pedeutour, K. Radhakrishnan, H. Cramail, A. Deffieux, Single-site olefin polymerization catalysts via the molecular design of porous silica, Macromol. Rapid Commun., 22 (2001) 1095-1123.

[11] P. Manisankar, A. Gomathi, D. Velayutham, Oxygen reduction at the surface of glassy carbon electrodes modified with anthraquinone derivatives and dyes, J. Solid State Electrochem., 9 (2005) 601-608.

[12] A. Rios-Escudero, M. Villagran, F. Caruso, J.P. Muena, E. Spodine, D. Venegas-Yazigi, L. Massa, L.J. Todaro, J.H. Zagal, G.I. Cardenas-Jiron, M. Paez, J. Costamagna, Electrocatalytic reduction of carbon dioxide induced by bis(*N*-R-2-hydroxy-1-naphthaldiminato)-copper(II) (R = *n*-octyl, *n*-dodecyl): Magnetic and theoretical studies and the X-ray structure of bis(*N*-*n*-octyl-2-hydroxy-1-naphthaldiminato)-copper(II),Inorg. Chimi. Acta., 359 (2006) 3947-3953.

[13] A. Ourari, Y. Ouennoughi, D. Aggoun, M. S. Mubarak, E. M. Pasciak, D. G. Peters, Synthesis, characterization, and electrochemical study of a new tetradentate nickel(II)-Schiff base complex derived from ethylenediamine and 5′-(*N*-methyl-*N*-phenylaminomethyl)-2′-hydroxyacetophenone,Polyhedron, 67 (2014) 59-64.

[14] A. Ourari, D. Aggoun, L. Ouahab, A novel copper(II)-Schiff base complex containing pyrrole ring: Synthesis, characterization and its modified electrodes applied in oxidation of aliphatic alcohols, Inorg. Chem. Commun., 33 (2013) 118-124.

View Article Online
DOI: 10.1039/C5RA10819E

[15] C. P. Horwitz and R.W. Murray, Oxidative Electropolymerization of Metal Schiff Base Complexes, Mol. Cryst. Liq. Cryst., 160 (1988) 389-404.

[16] S. Kannan, M. Sivagamasundari, R. Ramesh, Yu Liu, Ruthenium(II) carbonyl complexes of dehydroacetic acid thiosemicarbazone: Synthesis, structure, light emission and biological activity, J. Organomet. Chem., 693 (2008) 2251-2257.

[17]A. Altomare, M. C. Burla, M. Camalli, G. Cascarano, C. Giacovazzo, A. Guagliardi, A. G. G. Moliterni, G. Polidori, R. Spagna, SIR97: a new tool for crystal structure determination and refinement, J. Appl. Cryst. (1999) 32, 115-119

[18] G.M. Sheldrick, A short history of SHELX, Acta.Cryst. A64 (2008), 112-122

[19]L. J. Farrugia, WinGX and ORTEP for Windows: an update, J. Appl. Cryst., 45 (2012) 849-854

[20] K. Nakamoto, Infrared and Raman Spectra of Inorganic and Coordination Compounds, sixth ed., John Wiley & Sons, Inc., New Jersey (2009).

[21]M. Morshedi, M. Aminasr, A.M.Z. Slawin, J.D. Woollins, A.D. Khalaji, Synthesis and coordination chemistry of new tetradentate N_2S_2 donor Schiff-base ligand ca_2-dapte: Mononuclear and dinuclear copper(I) complexes $[Cu(ca_2dapte)]ClO_4$ and $[\{Cu(PPh_3)(X)\}_2(ca_2dapte)]$ (X = I and Br), Polyhedron, 28 (2009) 167-171.

[22] K. Nakamoto, Infrared and raman spectra of inorganic and coordination compounds, part B: Applications in coordination, organometallic, and bioinorganic chemistry. Wiley: New York (1997).

[23]B. Samanta, J. Chakraborty, C. R. Choudhury, S. K. Dey, D. K. Dey, S. R. Batten, P. Jensen, Glenn P. A. Yap, S. Mitra, New Cu(II) complexes with polydentate chelating Schiff base ligands: Synthesis, structures, characterizations and biochemical activity studies, Struct. Chem., 18 (2007) 33-41.

[24]X.-H. Lu, Q.-H. Xia, H.J. Zhan, H.X. Tuan, C.P. Ye, K.X. Su, G. Xu, Synthesis, characterization and catalytic property of tetradentate Schiff-base complexes for the epoxidation of styrene, J. Mol. Catal. A: Chem., 250 (2006) 62-69.

[25]F. Karipcin, B. Dede, S. Percin-Ozkorucuklu, E. Kabalcilar, Mn(II), Co(II) and Ni(II) complexes of 4-(2-thiazolylazo)resorcinol: Syntheses, characterization, catalase-like activity, thermal and electrochemical behaviour, Dyes and Pigments, 84 (2010) 14-18.

[26] R. Bikas, H. H. Monfared, T.Lis, M.Siczek, Synthesis, structural characterization and electrochemical studies of an ionic cobalt complex derived from a tridentate hydrazone Schiff base and azide ligands, Inorg. Chem. Commun., 15 (2012) 151-155.

View Article Online
DOI: 10.1039/C5RA10819E

[27] P. Talukder, S. Shit, A. Sasmal, S. R. Batten, B. Moubaraki, K. S. Murray, S. Mitra, An antiferromagnetically coupled hexanuclear copper(II) Schiff base complex containing phenoxo and dicyanamido bridges: Structural aspects and magnetic properties, Polyhedron,30 (2011) 1767–1773.

[28]S. Gupta, S. Pal, A. K. Barik, A. Hazra, S. Roy, T. N. Mandal, S-M. Peng, G-H. Lee, M. S. E. Fallah, J. Tercero, S. K. Kar, Synthesis, characterization and magneto structural correlation studies on three binuclear copper complexes of pyrimidine derived Schiff base ligands, Polyhedron, 27 (2008) 2519-2528.

[29]A.W. Addison, T. N. Rao, J. Reedijk, J.V. Rijn G. C. Vershoor, Synthesis, structure, and spectroscopic properties of copper(II) compounds containing nitrogen–sulphur donor ligands; the crystal and molecular structure of aqua[1,7-bis(*N*-methylbenzimidazol-2′-yl)-2,6-dithia heptane] copper(II) perchlorate, Dalton Trans. (1984) 1349–1356.

[30] J.T. Lundquist, J.R. and R. S. Nicholson, Theory of the potential step-linear scan electrolysis method with a comparison of rate constants determined electrochemically and by classical methods, J. Electroanal. Chem., 16 (1968) 445-456.

[31]A. H. Kianfar, S. Ramazani, R. Hashemi Fath, M. Roushani, Synthesis, spectroscopy, electrochemistry and thermogravimetry of copper(II) tridentate Schiff base complexes, theoretical study of the structures of compounds and kinetic study of the tautomerism reactions by ab initio calculations, Spectro. chim. Acta, Part A., 105 (2013) 374–382.

[32] K. Aoki, K. Tokuda, H. Matsuda, Theory of linear sweep voltammetry with finite diffusion space, J. Electroanal. Chem., 146 (1983) 417-424.

[33] K. Aoki, K. Tokuda, H. Matsuda, Theory of linear sweep voltammetry with finite diffusion space: Part II. Totally irreversible and quasi-reversible cases, J. Electroanal. Chem., 160 (1984) 33-45.

[34] D. Benito, J.J. Garcıa-Jareno, J. Navarro-Laboulais, F. Vicente, Electrochemical behaviour of poly(neutral red) on an ITO electrode, J. Electroanal. Chem., 446 (1998) 47-55.

[35] A. Ourari, D. Aggoun, L. Ouahab, Poly(pyrrole) films efficiently electrodeposited using new monomers derived from 3-bromopropyl-*N*-pyrrol and dihydroxyacetophenone—Electrocatalytic reduction ability towards bromocyclopentane, Colloids and Surfaces A: Physicochem. Eng. Aspects, 446 (2014) 190-198.

[36]**(a)** C.C. Pla Cid, E.R. Spada, M.L. Sartorelli, Effect of the cathodic polarization on structural and morphological proprieties of FTO and ITO thin films,Appl. Surf. Sci., 273 (2013) 603-606; **(b)** A.P. Moura, L.S. Cavalcante, J.C. Sczancoski, D.G. Stroppa, E.C. Paris, A.J. Ramirez, J.A. Varela, E. Longo, Structure and growth mechanism of CuO plates obtained

View Article Online
DOI: 10.1039/C5RA10819E

by microwave-hydrothermal without surfactants, Advanced Powder Technology 21 (2010) 197–202.

[37] X. Zhang, G. Wang, X. Liu, H. Wu, B. Fang, Copper Dendrites: Synthesis, Mechanism Discussion, and Application in Determination of L-Tyrosine, Cryst. Growth. Dyes., 8 (2008) 1430-1434.

[38] D.K. Sarkar, X.I. Zhou, A. Tannous, K.T. Leung, Growth Mechanisms of Copper Nanocrystals on Thin Polypyrrole Films by Electrochemistry, J. Phys. Chem. B 107 (2003) 2879-2881.

[39] S. H. Kazemi, R. Mohamadi, Electrochemical fabrication of a novel conducting metallopolymer nanoparticles and its electrocatalytic application, Electrochim. Acta, 109 (2013) 823-827.

[40] M. S. Ureta-Zanartu, C. Berrıos, J. Pavez, J. Zagal, C. Gutierrez, J. F. Marco, Electrooxidation of 2-chlorophenol on polyNiTSPc-modified glassy carbon electrodes, J. Electroanal. Chem. 553 (2003) 147-156.

[41] P. Wang, D. Zhang, R. Qiu, J. Wu, Super-hydrophobic metal-complex film fabricated electrochemically on copper as a barrier to corrosive medium, Corrosion Science, 83 (2014) 317–326.

[42] G. Costa, A. Puxeddu, E. Reisenhofer, Reactions of cobalt(I) complexes with ammonium and sulphonium ions and organic halides J. Chem. Soc. Dalton Trans., (1973) 2034-2039.

[43] M.P. Foley, P. Du, K.J. Griffith, J. A. Karty, M. S. Mubarak, K. Raghavachari, D. G. Peters, Electrochemistry of substituted salen complexes of nickel(II): Nickel(I)-catalyzed reduction of alkyl and acetylenic halides, J. Electroanal. Chem., 647 (2010) 194–203.

[44] A. L. Guyon, L. J. Klein, D. M. Goken, D.G. Peters, Catalytic reduction of 1-bromooctane by nickel(I) salen electrogenerated at a mercury cathode in dimethylformamide, J. Electroanal. Chem., 526 (2002) 134–138.

[45] D. Bhattacharya, M. J. Samide, Dennis G. Peters, Catalytic reduction of cyclohexane-carbonyl chloride with electrogenerated nickel(I) salen in acetonitrile, J. Electroanal. Chem., 441 (1998) 103-107.

[46] P.W. Raess, M.S. Mubarak, M.A. Ischay, M.P. Foley,T.B. Jennermann, K. Raghavachari, D.G. Peters, Catalytic reduction of 1-iodooctane by nickel(I) salen electrogenerated at carbon cathodes in dimethylformamide: Effects of added proton donors and a mechanism involving both metal- and ligand-centered one-electron reduction of nickel(II) salen, J. Electroanal. Chem., 603 (2007) 124–134

View Article Online
DOI: 10.1039/C5RA10819E

[47] P.C. Gach, J. A. Karty, D. G. Peters, Catalytic reduction of hexachlorobenzene and pentachlorobenzeneby cobalt(I) salen electrogenerated at vitreous carbon cathodes in dimethylformamide, J. Electroanal. Chem., 612 (2008) 22–28

[48] Z. Galus, Fundamentals of Electrochemical Analysis, Ellis Horwood, New York, NY, 1976.

List of captions

Scheme:

Scheme 1. Reaction way leading to the formation of the Schiff base copper (II) complex.

Scheme 2. Proposed yields for electroreduction of bromocyclopentane [46].

Scheme 3. Mechanism for electroreduction of bromocyclopentane proposed by P.W. Raess *et al.* [46].

Scheme 4. Mechanism for electroreduction of iodobenzene proposed by P.C. Gach *et al.* [47].

Figures:

Fig. 1 ORTEP drawing of the complex with atomic labelling, 50% ellipsoid probability.

Fig. 2 Cyclicvoltammograms recorded with 1mM of **Cu(L)(Py)(ClO_4)** in DMF solutions containing 0.1 M TBAP using 100 mVs^{-1} as scan rate going from: **(A)** +0.0 to +1.6 and **(B)** -0.2 to -1.6 V/SCE.

Fig. 3 Poly-**[Cu(L)(Py)(ClO_4)]** films obtained on GC electrode in DMF solutions, 0.1 M TBAP from -0.2 to +1.2 using 100 mV s^{-1} as scan rate **(A)** and then from 0 to -1.2 V/SCE **(B)** using 50 mV s^{-1} as scan rate.

Fig. 4 Cyclic voltammograms, recorded from DMF solutions 1 mM of copper (II) complex using a disc of GC as working electrode and 0.1 M TBAP with various scan rates going from

View Article Online
DOI: 10.1039/C5RA10819E

-0.2 to -1.6 V/SCE **(A)** and then, from 0.0 to -1.2 V/SCE **(B)** of **Cu(L)(Py)(ClO_4)** and poly-**[Cu(L)(Py)(ClO_4)]** respectively.

Fig. 5 Scanning electron micrographs of **Cu(L)(Py)(ClO_4)** complex deposited on ITO (**A**, **B**, **C** and **D**) and FTO (**E**, **F**, **G** and **H**) substrates.

Fig. 6 XPS spectra of Cu sample. (a) Survey spectra of **[Cu(L)(Py)(ClO_4)]** complex powder, (b) Survey spectra of poly-**[Cu(L)(Py)(ClO_4)]/ITO** films.

Fig. 7 Cyclic voltammograms, recorded at 100 mV s^{-1} for the electroreduction of bromocyclopentane on GC-electrode in DMF solutions containing 0.1 M TBAP in homogeneous phase (**A**), in heterogeneous phase (**B**) and for the electroreduction of iodobenzene (**C**).

Fig. 8 Cyclovoltammograms of poly-**[Cu(L)(Py)(ClO_4)]** recorded in presence of 5.10^{-3} M of iodobenzene at different scan rates:10, 25, 50,75, 100 mVs^{-1}.

Fig. 9 Chronoamperograms obtained for Two concentrations of iodobenzene solutions using **Cu(L)(Py)(ClO_4)** modified electrode, See curve (**A**); slope of $\mathbf{I_C / I_L}$ vs. $\mathbf{t^{1/2}}$ plot (**B**).

Tables:

Table 1. Crystal data and structure refinement for **Cu(L)(Py)(ClO_4).**

Table 2. Geometric parameters (Å, °): Selected bond lengths [Å] and angles [°].

View Article Online
DOI: 10.1039/C5RA10819E

Scheme 1:

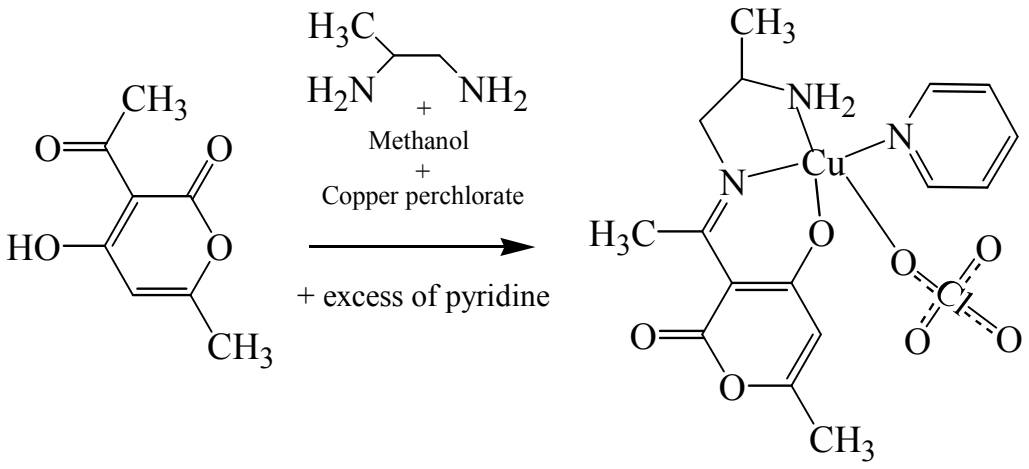

Scheme 2:

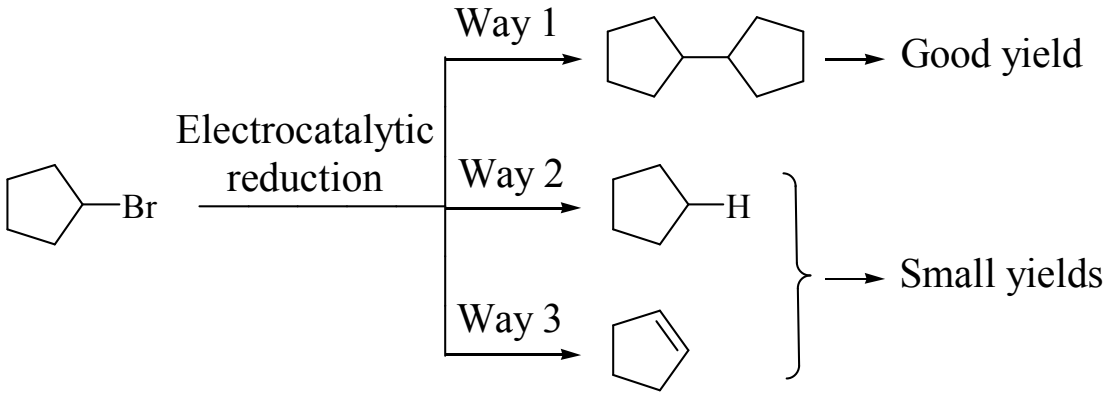

Scheme 3:

View Article Online
DOI: 10.1039/C5RA10819E

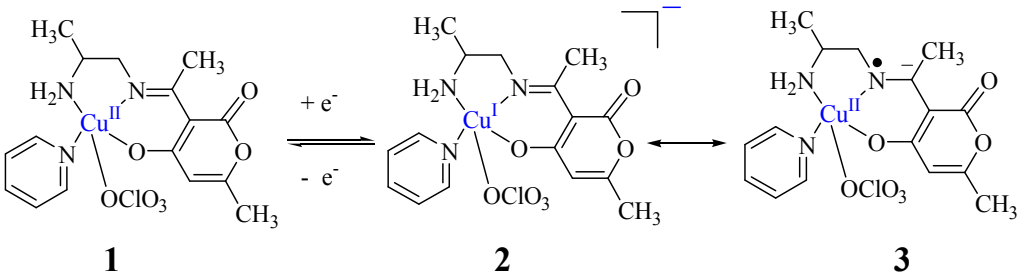

1 **2** **3**

(1) 2 (or 3) +  → 1 +  + Br^-

(2) 2  → 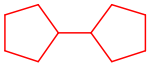

(3) 2  → 

(4) 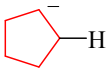 Solvant → 

(5)  Solvant → 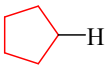

(6) 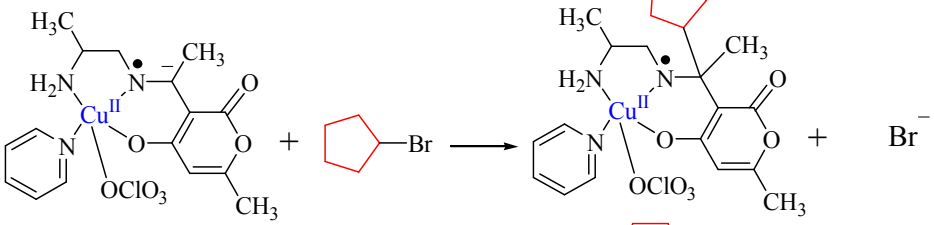

(7) 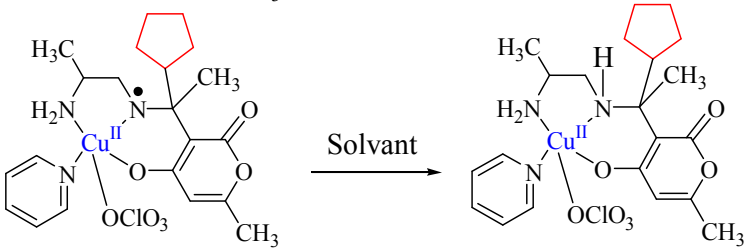

(8) 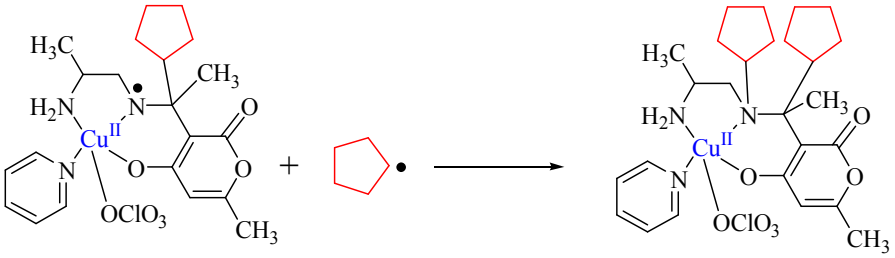

View Article Online
DOI: 10.1039/C5RA10819E

Scheme 4:

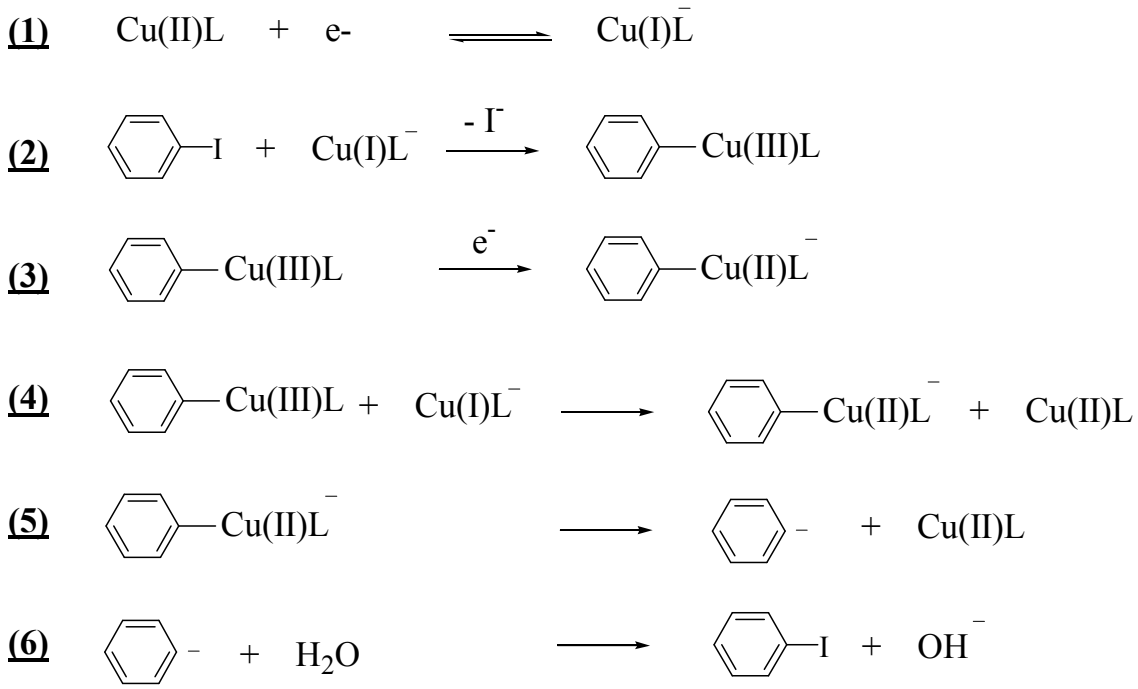

Fig. 1.

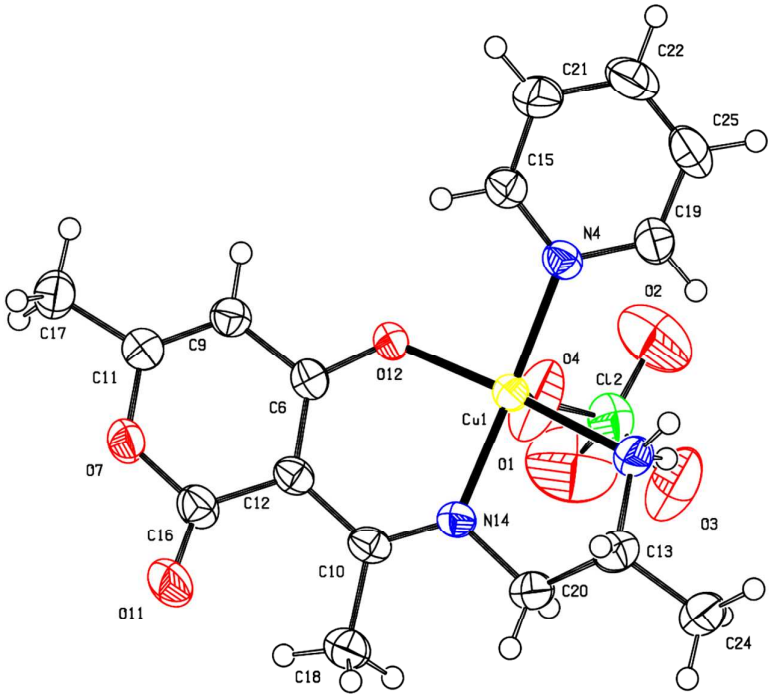

Fig. 2.

View Article Online
DOI: 10.1039/C5RA10819E

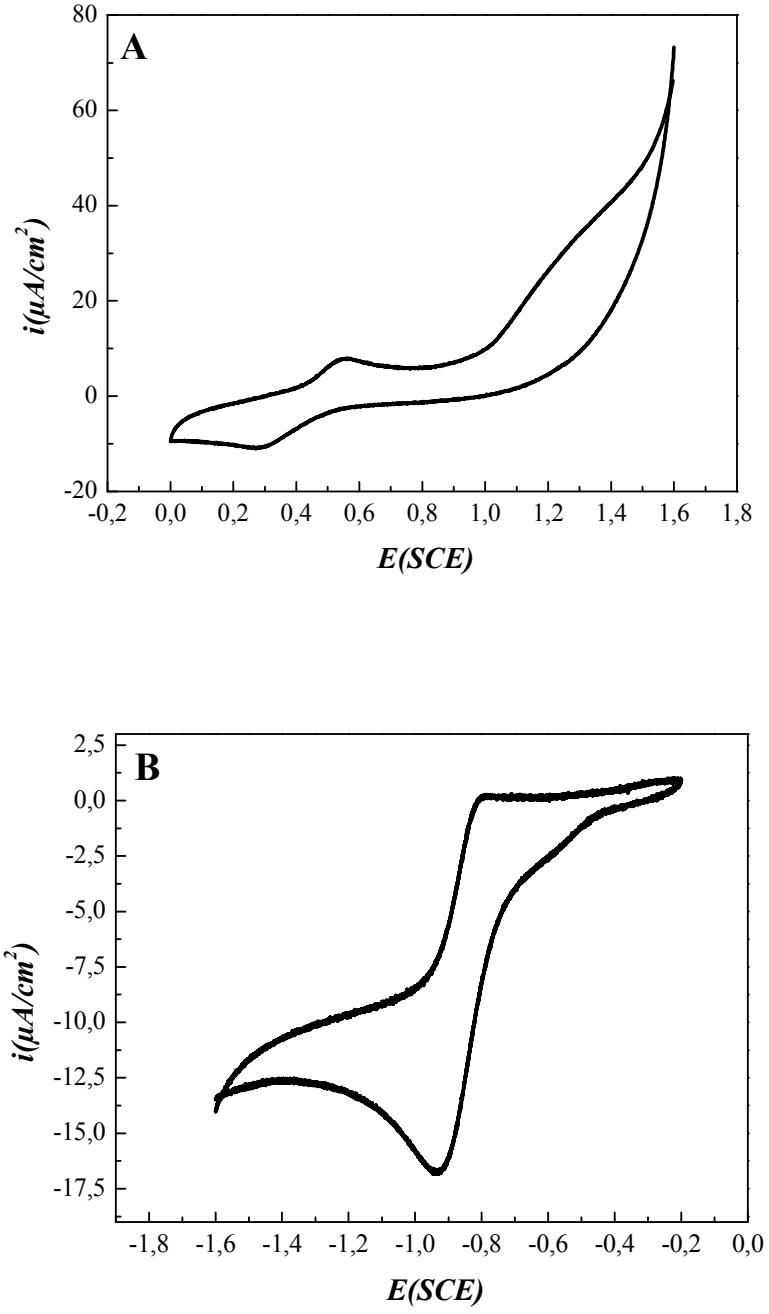

Fig. 3.

View Article Online
DOI: 10.1039/C5RA10819E

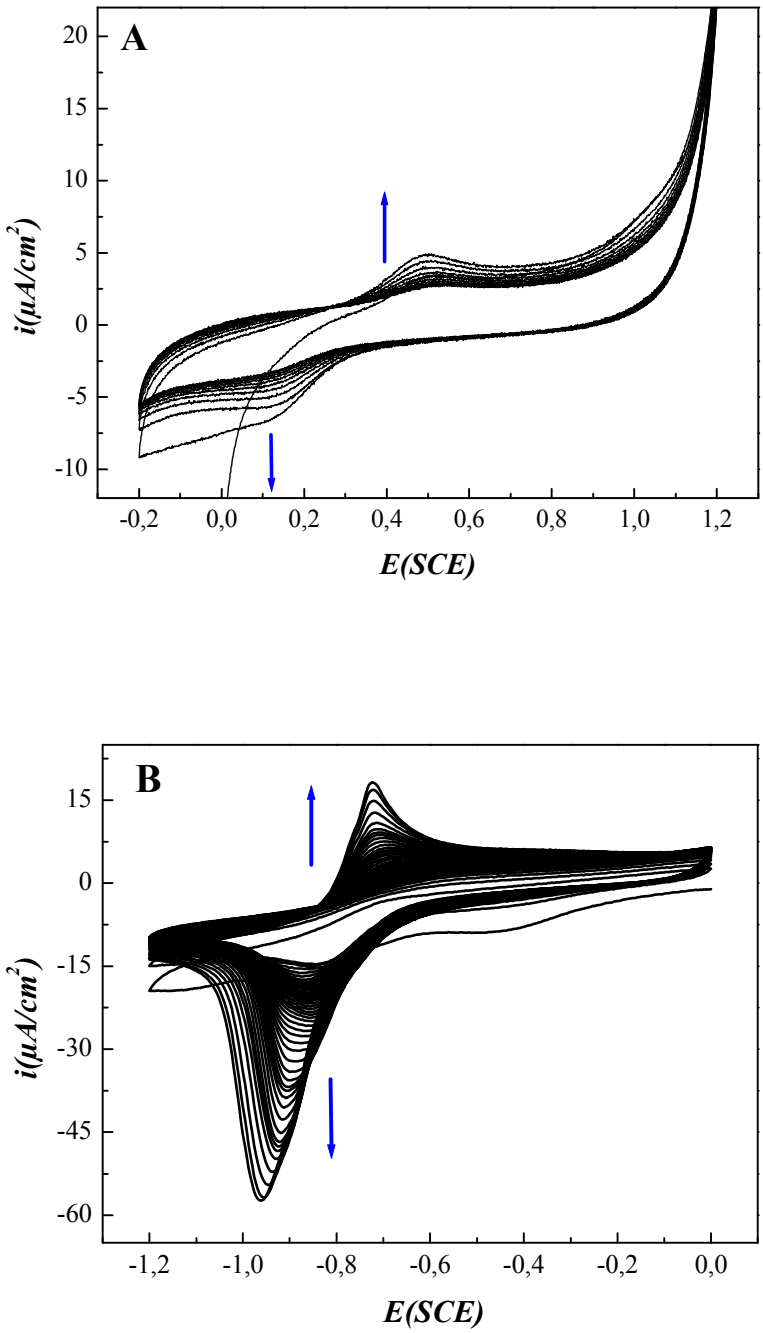

Fig. 4.

View Article Online
DOI: 10.1039/C5RA10819E

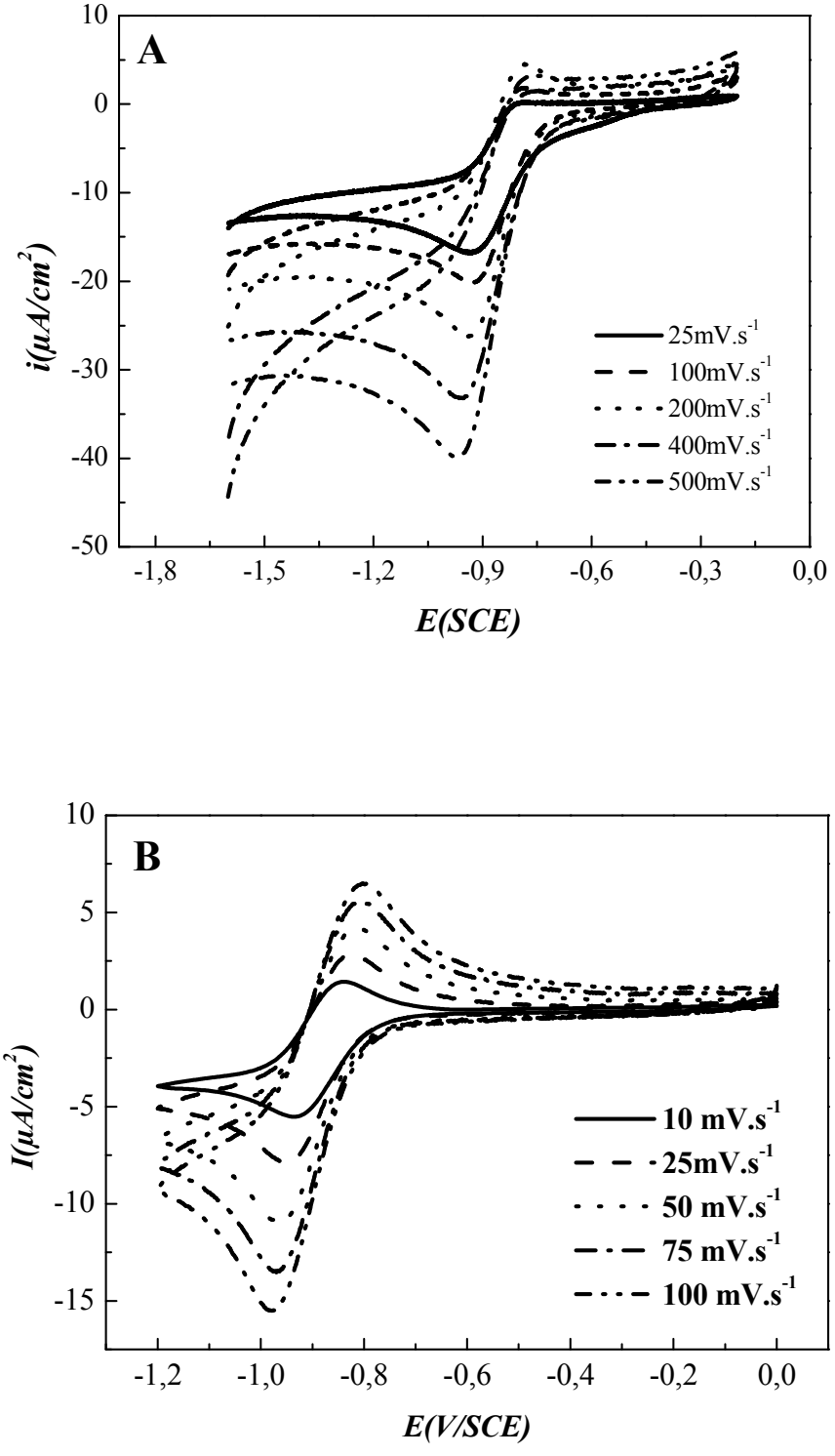

Fig. 5.

View Article Online
DOI: 10.1039/C5RA10819E

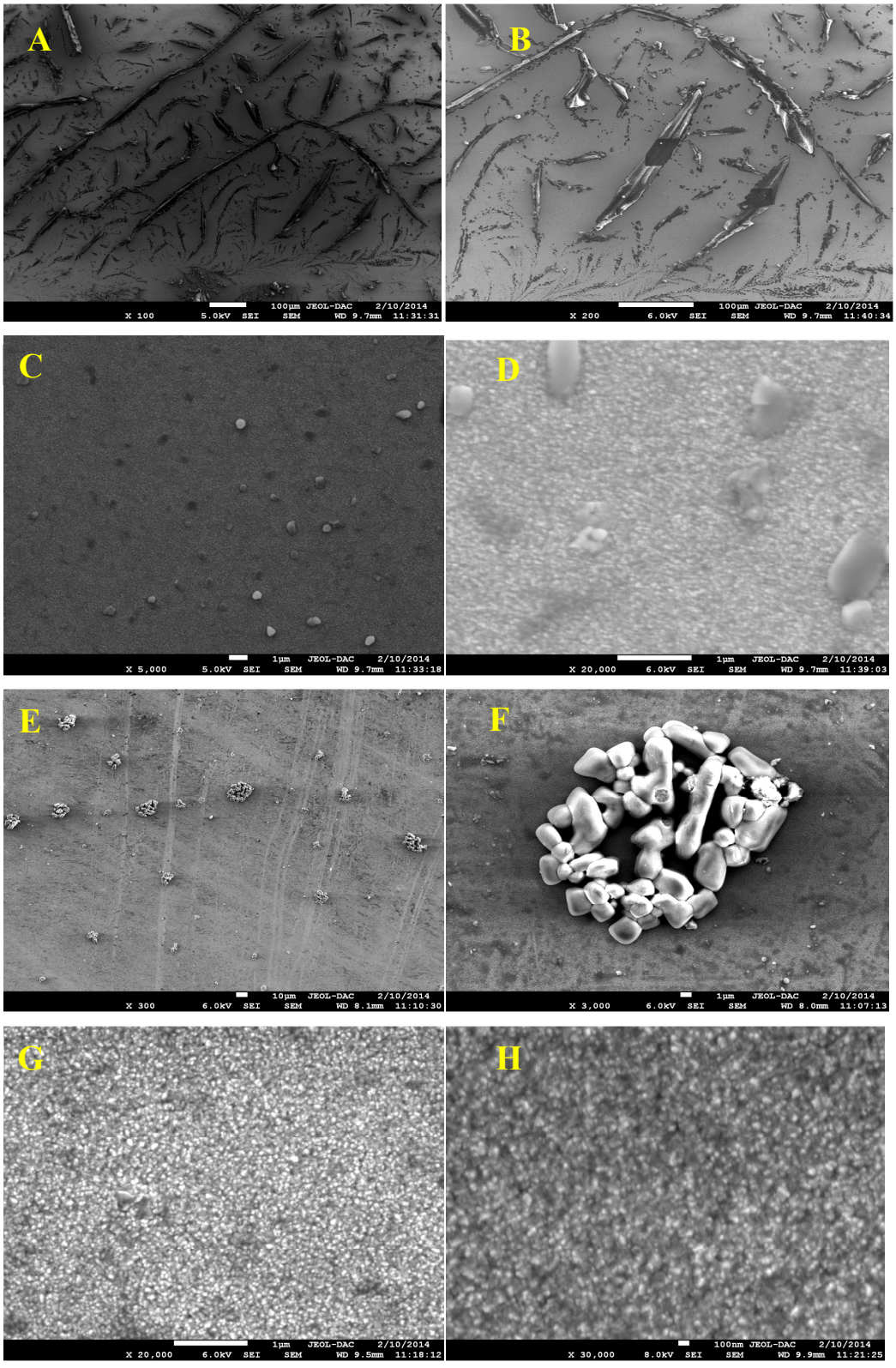

View Article Online
DOI: 10.1039/C5RA10819E

Fig. 6.

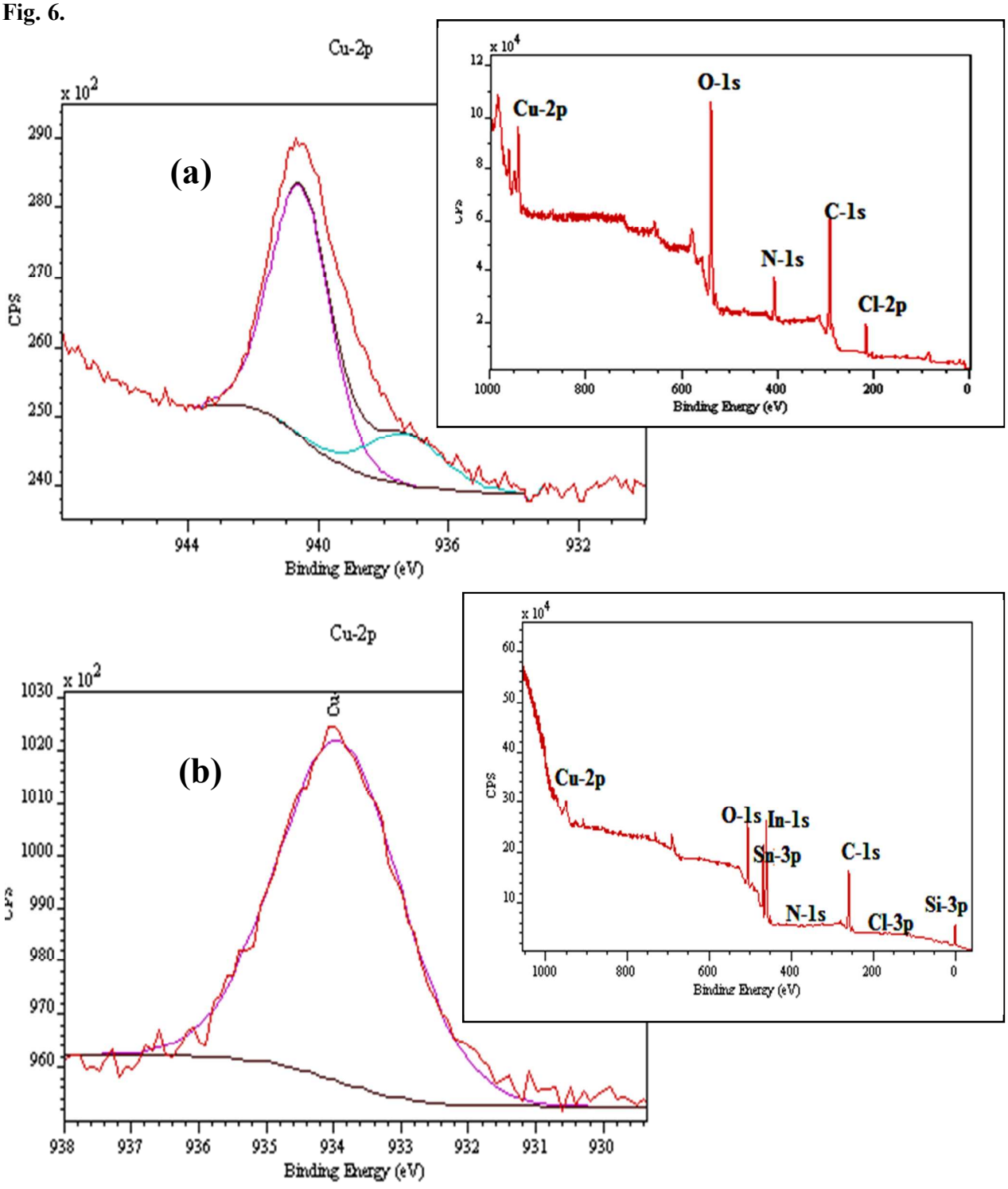

View Article Online
DOI: 10.1039/C5RA10819E

Fig. 7.

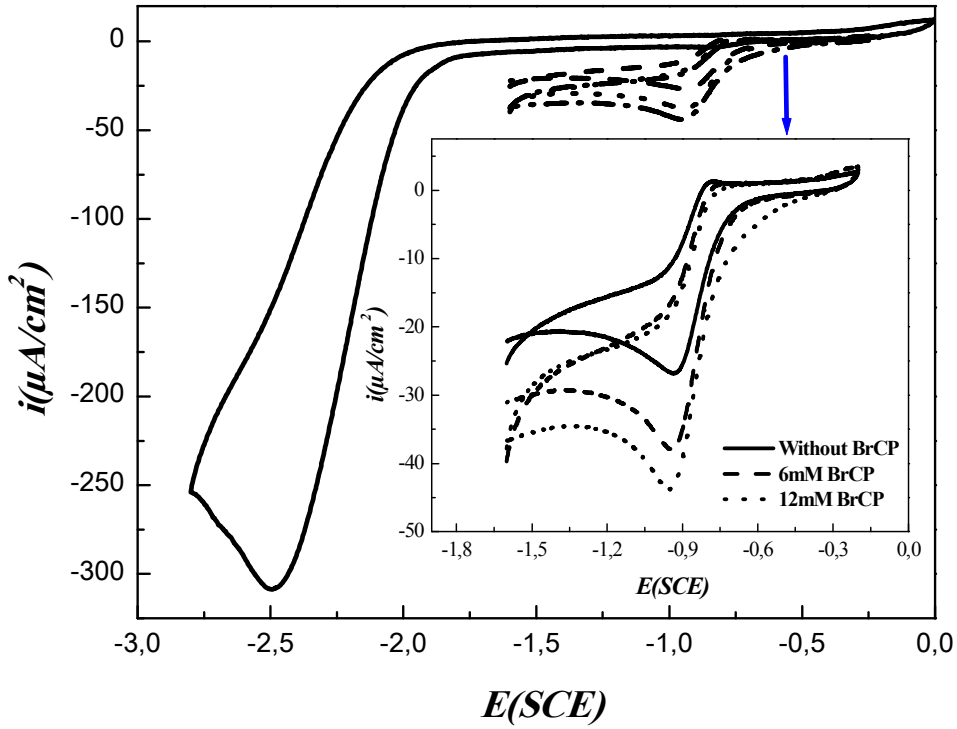

A

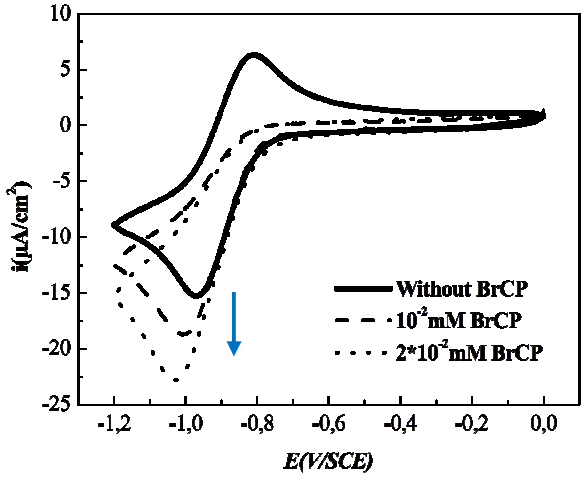

B

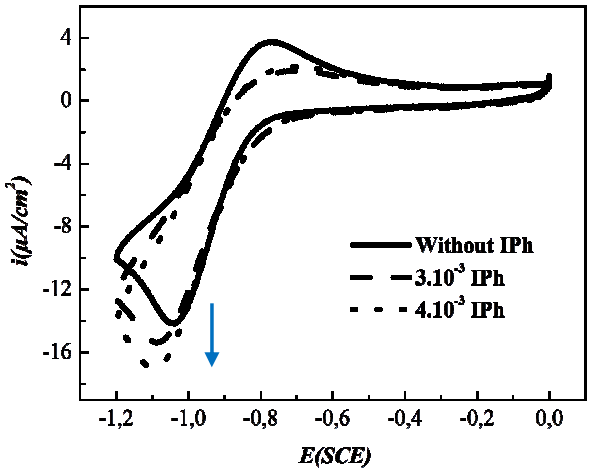

C

View Article Online
DOI: 10.1039/C5RA10819E

Fig. 8.

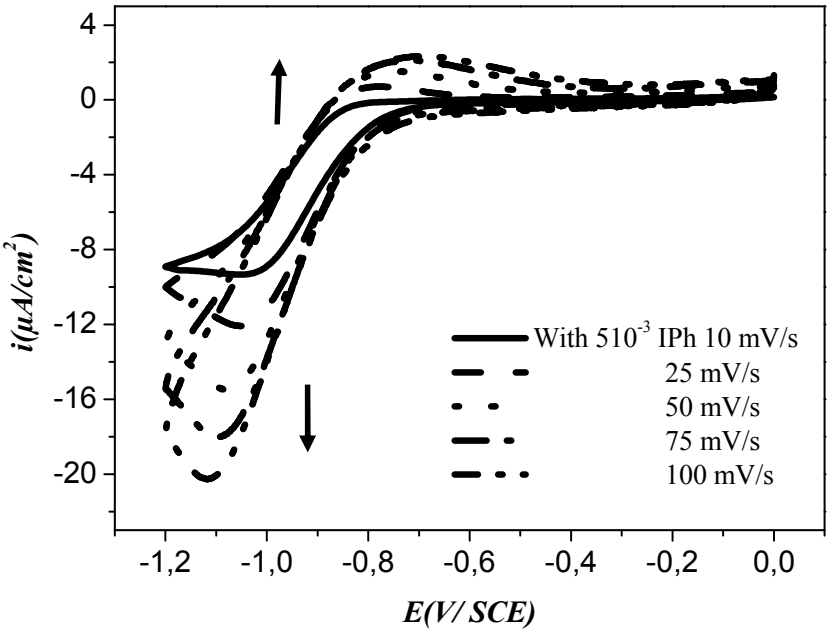

Fig. 9.

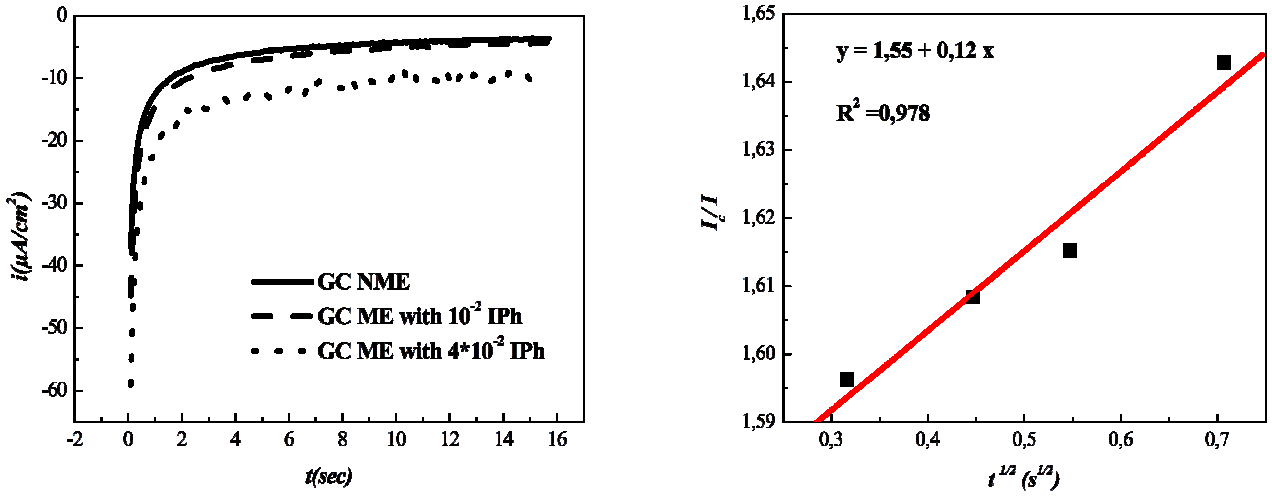

(A) **(B)**

Table 1.

View Article Online
DOI: 10.1039/C5RA10819E

Molecular formula	$C_{16}H_{20}CuN_3O_3{\cdot}ClO_4$
Molecular weight	465.34
Temperature (K)	293
Radiation λ	Mo-Kα (0.71073 Å)
Crystal system	Orthorhombic
Space group	-P 2bc 2ac
a/Å	11.051 Å
b/ Å	15.58 Å
c/ Å	21.736 Å
V/Å^3	3742.3 Å3
Z	8
Dcalc (g cm^{-3})	1.652
Crystal size (mm^3)	0.4 × 0.3 × 0.1
Crystal description	Prism
Crystal colour	Colourless
Absorption coefficient (mm-1)	1.36
F(0 0 0)	1912
Reflections collected	4288 [Rint = 0.064]
Range/indices (h, k, l)	−13,14; −20,20; −27,28
θ limit	3.6– 27.5
No. of observed data, I > 2σ (I)	3007
No. of variables	256
No. of restraints	0
Goodness of fit on F 2	0.125
Largest diff. Peak and hole (e Å-3)	0.57 and −0.42
R1 [I > 2<sigma>(I)]	0.0484
wR2	0.1245

$$R = \{\Sigma[w(|F0| - |Fc|)]/ \Sigma\, w(|F0|)\},\ Rw = \{\Sigma[w(|F0| - |Fc|)^2]/\Sigma\, w(|F0|^2)\}^{1/2},$$

$$wR2 = \{\Sigma[w(F0^2 - Fc^2)^2]/ \Sigma\, w(F0^2)\}^{1/2}$$

$w = 1/[\sigma^2(F_o^2) + (0.0794P)^2 + 0.6853P]$ where $P = (F_o^2 + 2F_c^2)/3$.

Table 2.

Cu1—O12	1.901 (2)	**N13—Cu1—N4**	95.38 (11)
Cu1—N14	1.970 (3)	**C6—O12—Cu1**	128.6 (2)
Cu1—N13	1.991 (3)	**C15—N4—Cu1**	121.2 (2)
Cu1—N4	2.036 (3)	**C19—N4—Cu1**	122.1 (2)
O12—Cu1—N14	90.77 (10)	**C10—N14—Cu1**	128.8 (2)
O12—Cu1—N13	174.51 (11)	**C20—N14—Cu1**	110.1 (2)
N14—Cu1—N13	85.43 (11)	**C13—N13—Cu1**	108.7 (2)
O12—Cu1—N4	88.87 (10)	**Cu1—N13—H13A**	110
N14—Cu1—N4	172.95 (11)	**Cu1—N13—H13B**	110